ACOUSTICS 2012

Reproduction of random acoustic pressure fields on plane surfaces using wave field synthesis and planar holography

O. Robin, A. Berry, S. Moreau and R. Dia

GAUS, Université de Sherbrooke - 2500, Bd de l'Université, Sherbrooke, Canada J1K 2R1
olivier.robin@usherbrooke.ca

Vibroacoustic testing of many panel structures such as building partitions, automotive windscreens or fuselage panels, is often performed in coupled reverberant - anechoic rooms under Diffuse Acoustic Field (DAF) assumption. However, an ideal and repeatable DAF is difficult to reach in practice, especially at low frequencies. Moreover, DAF excitation does not reflect the actual Transmission Loss (TL) of structural parts of a moving vehicle, subjected to complex wall pressure fluctuations related to Turbulent Boundary Layer (TBL) excitation developing on its external surface. Experiments under TBL excitation can be performed using wind tunnels or in-vehicle testing, but such measurements are time consuming, costly and show discrepancies. Two sound field reproduction strategies, Wave Field Synthesis and Planar Near Field Holography, are proposed here to perform robust laboratory reproduction of DAF and TBL pressure fields in 2-D (i.e. sound pressure distribution on a plane surface), which are defined using their Cross-Spectral Densities (CSD) or wavenumber–frequency spectrum. Numerical simulations of reproduction frameworks are performed for acoustic monopoles as reproduction sources, distributed on a plane facing a virtual panel to be tested. Synthesis results are then analyzed in both spatial and wavenumber domains, and compared to other works. Finally, recommendations for a practical implementation are presented.

1 Introduction

Many structures can be exposed to wall pressure fluctuations caused by their motion in a fluid (ship hull, aircraft fuselage), which can contribute to the acoustic radiation of these structures and thus to interior noise levels. These wall pressure fluctuations are composed of a turbulent component and an acoustic component, with different characteristics. For example, the ratios between their spectral levels are roughly ranging from 10 to 30 dB [1, 2], which lead to a problematic imprecision concerning the roles of these two components. Therefore there is a crucial need to be able to perform robust experimental measurements of panel TL under DAF and TBL excitations.

The earliest works on TBL reproduction (see Refs. 29 and 30 in [3]) were published in the 1960s, and established the feasibility of such reproduction. Few works have been conducted then until the 2000s. Between 2000 and 2010, many studies have been published by Maury and Bravo *et al* (see Refs. 32 to 37 in [3]) on the reproduction of TBL excitation using a nearfield array of loudspeakers, with the most recent work published in 2011 [4]. Their approach is based on a close-loop scheme, with a necessary measurement of surface pressure and related signal processing. Aucejo *et al* [5] suggested the use of a synthetic antenna towards this goal, which simplifies some technical constraints. It nevertheless implies to *a priori* measure transfer functions between the acoustic sources and the reproduction surface to prevent ill-conditioning when determining the inputs to the acoustic reproduction sources.

Recently, Berry *et al* [3] proposed an open-loop method for the reproduction of spatially-correlated sound fields, based on Wave Field Synthesis (WFS). In this paper, this WFS approach is shortly presented, and another open-loop method based on Planar Nearfield Acoustical Holography (P-NAH) is introduced. Figure 1 simply illustrates the problem under study. Given a pressure distribution to synthetize on a plane S_1 (*reproduction plane*), WFS and P-NAH are used to impose particle velocity to acoustic sources (idealized monopoles) distributed on a plane S_2 (*source plane*) facing S_1, so that the sound pressure distribution is effectively reproduced on S_1. The plane S_1 is considered acoustically transparent, and free-field conditions are assumed.

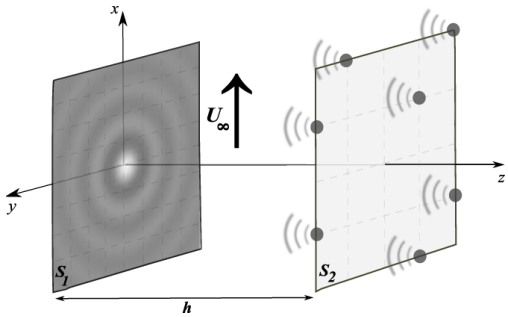

Figure 1: Problem geometry and coordinate system – The free-flow direction is indicated by the bold vertical arrow for the TBL case (U_∞ is the free-flow speed) – h is the distance separating the two planes – Illustrated CSD on plane S_1 corresponds to a DAF.

2 Spatially Correlated Sound Fields

The two random pressure fields of interest must be described using statistical properties such as the Cross-Spectral Density (CSD) $S_{pp}(\mathbf{r_1}, \mathbf{r'_1}; \omega)$ which gives the correlation in the spectral domain between two arbitrary points (located by vectors $\mathbf{r_1}$ and $\mathbf{r'_1}$ in the plane S_1 – in this paper, any presented CSD is calculated between the center of the surface and a variable point). The wavenumber-frequency spectrum $S_{pp}(\mathbf{k}; \omega)$, the 2D spatial Fourier transform of the CSD function is also used. Both random processes are assumed to be spatially homogeneous and temporally stationnary.

2.1 Diffuse Acoustic Field

The CSD of an DAF can be written [1]

$$S_{pp}(\mathbf{r_1}, \mathbf{r'_1}; \omega) = S_{pp}(\omega) \frac{\sin k_0 |\mathbf{r_1} - \mathbf{r'_1}|}{k_0 |\mathbf{r_1} - \mathbf{r'_1}|}. \tag{1}$$

The wavenumber-frequency spectrum is expressed as [1]

$$S_{pp}(\mathbf{k}; \omega) = \begin{cases} \frac{S_{pp}(\omega)}{2\pi k_0^2} \frac{1}{\sqrt{1-(|\mathbf{k}|/k_0)^2}} & \text{if} \quad |\mathbf{k}| < k_0, \\ 0 & \text{if} \quad |\mathbf{k}| > k_0, \end{cases} \tag{2}$$

where $|\mathbf{k}| = \sqrt{k_x^2 + k_y^2}$, and the autospectrum $S_{pp}(\omega)$ being considered here unitary. Theoretical DAF corresponds to the summation of uncorrelated acoustic plane waves propagating at the speed of sound c_0 and equally distributed in space at a given frequency (with the acoustic wavenumber $k_0 = \omega/c_0$ and ω the angular frequency). Figure 2-a illustrates the theoretical CSD of a DAF. Figure 2-b gives the corresponding

CSD wavenumber spectrum. In the plane (k_x, k_y), the spectrum has the shape of a circle of radius k_0, named acoustic circle.

2.2 Turbulent Boundary Layer

As for DAF, the wall pressure fluctuations related to TBL excitation can be theoretically described by a summation of uncorrelated plane waves [5]. Compared to DAF, the wavenumber spectrum of TBL is not purely limited to the acoustic circle, is highly anisotropic and its shape is mainly defined by the convection speed U_c. U_c determines the energy peak of a TBL (the convective peak) located at the convective wavenumber $k_c = \omega/U_c$ in the flow direction, here k_x (the spectrum in the k_y direction is symmetric around $k_y = 0$).

Among many wall pressure fluctuations models that have been proposed since the 1950s for TBL, the simple empirical model of Corcos [6] is used here. The CSD given by the Corcos model is

$$S_{pp}(\mathbf{r_1}, \mathbf{r'_1}, \omega) = S_{pp}(\omega) e^{-\frac{\omega|\xi_{x_1}|}{\alpha U_c}} e^{-\frac{\omega|\xi_{y_1}|}{\beta U_c}} e^{j\frac{\omega(\xi_{x_1})}{U_c}}, \qquad (3)$$

where $S_{pp}(\omega)$ is the autospectrum of the pressure field (supposed unitary as for DAF), U_c the convection speed, $\xi_{x_1} = x_1 - x'_1$ and $\xi_{y_1} = y_1 - y'_1$ are longitudinal and transverse separations respectively. The coefficients α et β describe spatial correlation decays in the streamwise and crosswise directions respectively (values of $\alpha = 8$ and $\beta = 1.2$ are used in this paper). The convection speed U_c will be assumed to be constant with respect to frequency and is given by $U_c = 0.7U_\infty$. The wavenumber-frequency spectrum of the Corcos model is [6]

$$S_{pp}(k_x, k_y, \omega) = S_{pp}(\omega) \frac{\alpha\beta}{\left[1 + \alpha^2\left(1 - \frac{k_x}{k_c}\right)^2\right]\left[1 + \beta^2\left(\frac{k_y}{k_c}\right)^2\right]}. \qquad (4)$$

Figures 2-c,e illustrate the CSD of the Corcos model for a supersonic case and a subsonic case. Figures 2-d,f illustrate the corresponding wavenumber-frequency spectra. Note that when the TBL is supersonic, $k_c < k_0$ and dominant spatial correlation scales of the TBL are larger than half an acoustic wavelength. Inversely, when the TBL is subsonic, $k_c > k_0$ and dominant spatial correlation scales of the TBL are now significantly smaller than half an acoustic wavelength.

3 Sound Field Reproduction Techniques

3.1 Wave Field Synthesis

Wave Field Synthesis (WFS) is a sound field reproduction technique based on the Huygens principle, with the central idea of reproducing a wavefront radiated by a primary source with an array of secondary sources [7]. Theoretical approach uses Kirchhoff-Helmholtz integral in order to define the pressure field on a surface S_2 (where reproduction sources are distributed), given a target pressure field on surface S_1 (defined by equations 1 or 3 for example). The particle velocity field of sources is deduced with the Euler equation, the finally reproduced sound field on S_1 being calculated with Rayleigh's integral [3].

3.2 Nearfield Acoustic Holography

Nearfield Acoustical Holography (NAH) is widely used as a measurement technique for the prediction of acoustical quantities on a surface, using acoustical quantities generally measured on a parallel surface [8]. Even if Gabor named its invention in optics *wavefront reconstruction*, NAH is rarely used as a sound field reproduction technique. The fundamental relations of P-NAH are here used to propagate a pressure distribution to reproduce from the reproduction plane S_1 to the source plane S_2, and to derive the particle velocity to be imposed to acoustics sources distributed on S_2.

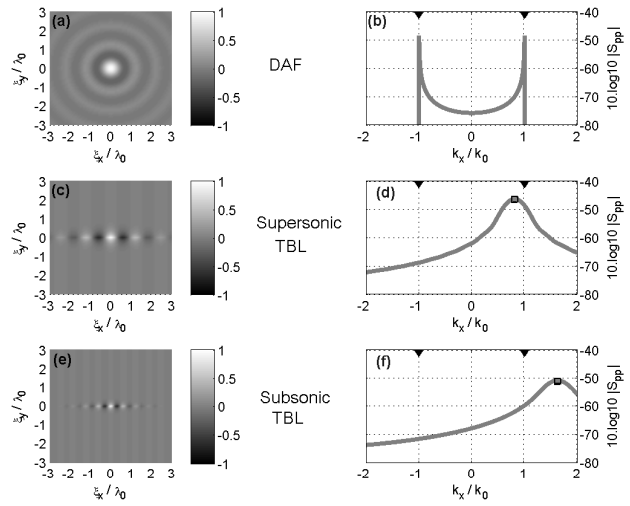

Figure 2: LEFT: Real part of the theoretical CSD for (a) DAF, (c) Supersonic TBL (U_∞ = 600 m/s) and (e) Subsonic TBL (U_∞ = 300 m/s) *(spatial separations are normalized by the acoustic wavelength λ_0)* – RIGHT : Magnitude of the theoretical wavenumber-spectrum $|S_{pp}(k_x, 0)|$ for (b) DAF, (d) Supersonic TBL and (f) Subsonic TBL *(wavenumbers are normalized by the acoustic wavenumber k_0)* – Down triangles are limits of the acoustic domain, black square locates the dimensionless convective wavenumber k_c/k_0.

4 Simulation results

The simulations results presented in this section are obtained with reproduction and sources planes of identical dimensions ($[-3\lambda_0 : 3\lambda_0] \times [-3\lambda_0 : 3\lambda_0]$), separated by a distance $h = \lambda_0$ (other plane separations are presented for the DAF case). The spatial sampling for the source plane is $\lambda_0/2$, this value of two acoustic sources per acoustic wavelength normally preventing spatial aliasing in the acoustic domain [7]. In following figures, the target pressure field is always indicated with a bold grey line, whereas the reproduced pressure field is illustrated with a thin black line. For a better visualization of spatial results, scales are adjusted and given on the left y-axis for the target CSD, and on the right y-axis for the reproduced CSD. The presented results are all obtained with the P-NAH approach, except for figure 6. Specific results for the WFS approach can be found in [3].

4.1 Diffuse Acoustic Field reproduction

Figure 3-a compares the real part of the DAF target CSD and reproduced CSD, with a spatial structure clearly well reproduced compared to the target, but with slightly smaller amplitudes. The results in figure 3-b show that the repro-

duction of grazing plane waves (i.e. waves with wavenumber close to $\pm k_0$) implies that source and reproduction planes are not too much spaced compared to their respective sizes. As the planes separation h increases (keeping planes dimensions unchanged), the reproduced wavenumber content narrows because it becomes physically impossible to reproduce waves with grazing incidence and thus wavenumber values close to k_0 (with the consequence that reproduced field amplitudes become smaller). Obviously, a source plane smaller than the reproduction plane will also prevent the reproduction of grazing plane waves.

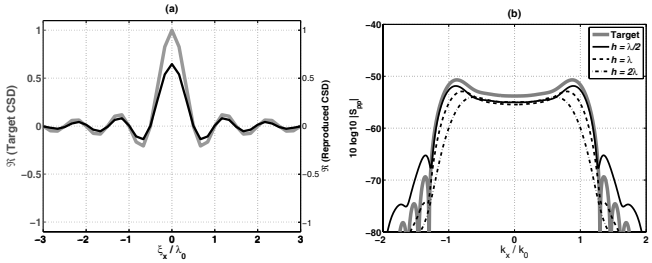

Figure 3: Reproduction of DAF – (a) Target CSD and reproduced CSD in the $(\xi_x, 0)$ plane - (b) Target CSD wavenumber-spectrum and reproduced CSD wavenumber spectrum in the $(k_x, 0)$ plane for various plane separations.

4.2 Supersonic and subsonic TBL reproduction

Results for the reproduction of a supersonic TBL are given in figure 4. In the streamwise direction, correlation scales are correctly reproduced (with a maximal reproduced amplitude which is nearly half the target one), but those in the crosswise direction are coarsely reproduced. Corresponding results in the wavenumber domain are also given in figures 4-c,d, showing that the target spectrum is clearly well reproduced inside the acoustic domain ($|\mathbf{k}|/k_0 \leq 1$). Note also in figure 4-c that a propagating phenomenon is clearly reproduced, with a highly asymmetric spectrum in k_x (the peak visible for $k_x/k_0 \approx -1$ is attributed to aliasing phenomenon in the wavenumber domain, due to the extension of the wavenumber content above k_0 [7]).

Figure 5 shows simulation results for a subsonic TBL. Compared to results in figure 4, two important observations can be made. First, the reproduced magnitudes in figures 5-a,b are significantly smaller than the target values, more than 25 times less. Second, target correlation scales are clearly not reproduced and have now the shape of those obtained in the case of DAF (see figure 3-a). Explanations are found in figures 5-c,d. As for the supersonic TBL, the target CSD wavenumber spectrum is clearly well reproduced inside the acoustic domain ($|\mathbf{k}|/k_0 \leq 1$) but the convective peak is now located outside this domain. Energy and correlation scales being driven by the convective peak, this explains small reproduced magnitudes and large reproduced correlations scales. The reproduced spectrum is slightly asymmetric in k_x (compared to the supersonic case) and symmetric along k_y (which partially explains the shape of the reproduced CSD in figure 5-a,b).

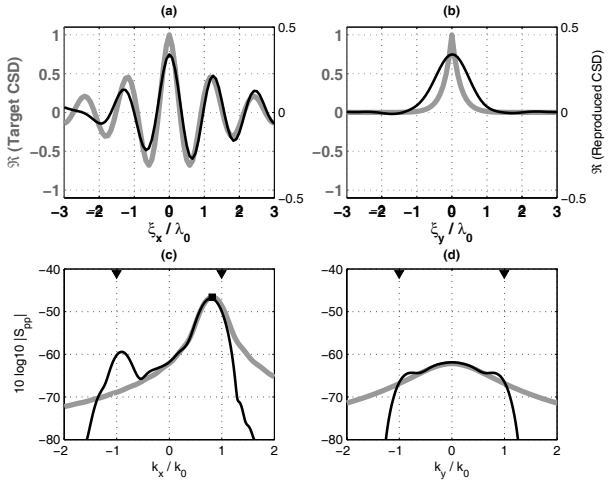

Figure 4: Supersonic TBL ($U_\infty = 600$ m/s) – Target CSD (bold gray line) and reproduced CSD in the $(\xi_x, 0)$ plane (a) and $(0, \xi_y)$ plane (b) – Target CSD wavenumber spectrum and reproduced CSD wavenumber spectrum in the $(k_x, 0)$ plane (c) and $(0, k_y)$ plane (d).

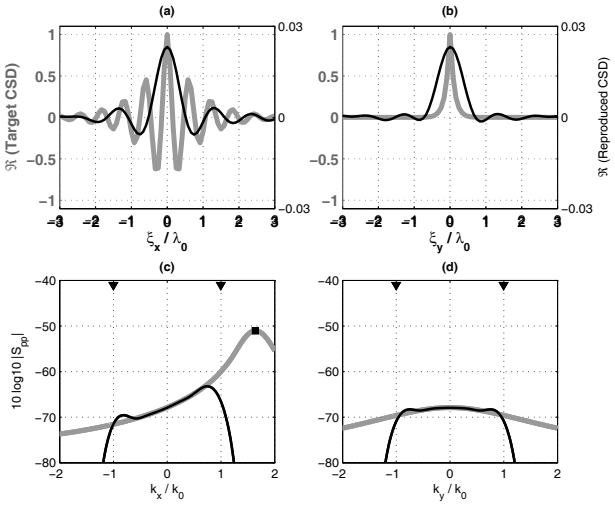

Figure 5: Subsonic TBL ($U_\infty = 300$ m/s) – Target CSD (bold gray line) and reproduced CSD in the $(\xi_x, 0)$ plane (a) and $(0, \xi_y)$ plane (b) – Target CSD wavenumber spectrum and reproduced CSD wavenumber spectrum in the $(k_x, 0)$ plane (c) and $(0, k_y)$ plane (d).

4.3 Reproduction error

The reproduction error is quantified by the difference between the target and reproduced sound pressure fields in the wavenumber domain, normalized by the target sound pressure field. The error can be calculated in the acoustic wavenumber domain only (denoted $\epsilon^0_{\hat{p}\hat{p}}$), or up to the convective wavenumber k_c (written $\epsilon^c_{\hat{p}\hat{p}}$ in this case), and is expressed as

$$\epsilon^{(0,c)}_{\hat{p}\hat{p}} = \frac{\int_{|\mathbf{k}|\leq(k_0,k_c)} |S_{pp}(\mathbf{k},\omega) - S_{\hat{p}\hat{p}}(\mathbf{k},\omega)|^2 d\mathbf{k}}{\int_{|\mathbf{k}|\leq(k_0,k_c)} |S_{pp}(\mathbf{k},\omega)|^2 d\mathbf{k}}, \qquad (5)$$

where $k_0 = \omega/c_0$ is the acoustic wavenumber and $k_c = \omega/U_c$ is the convective wavenumber. The reproduction errors in the acoustic domain $\epsilon^0_{\hat{p}\hat{p}}$ are compared with the WFS open-loop method [3] in figure 6. The sizes of source plane

and reproduction plane are identical to those given in the introductory paragraph of section 4.

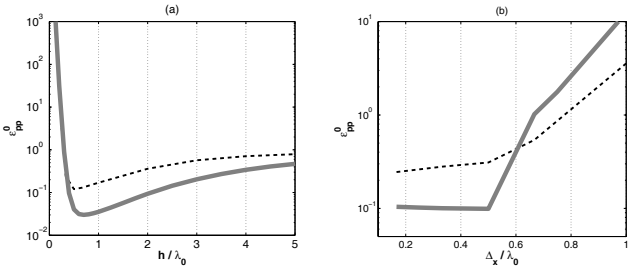

Figure 6: Comparison of reproduction error in the acoustic domain for a subsonic TBL, for P-NAH based approach (bold gray line) and WFS based approach (dashed thin black line) – (a) Influence of planes separation h and (b) Influence of reproduction sources separation Δ_x (both normalized by the acoustic wavelength λ_0).

The global trends are similar in both methods, with slightly better results for the P-NAH method for the tested configuration. For the error plotted as a function of plane separation in figure 6-a, the minimal reproduction error in the WFS approach is reached for a separation of $\lambda_0/2$, while the optimal separation distance is close to $3\lambda_0/4$ for the NAH approach. In figure 6-b, the P-NAH approach seems more sensitive to the sources discretization in plane S_2 (when less than two acoustic sources are used per acoustic wavelength ($\Delta_x/\lambda_0 > 0.5$), the error increase faster than for WFS). For both methods, the reproduction error is small and nearly constant with $\Delta_x/\lambda_0 < 0.5$, showing that having reproduction sources spaced by less than half an acoustic wavelength cannot be avoided in practice.

5 Parametric study in the NAH case

Values of the reproduction error are mapped as a function of planes separation and spatial sampling in the source plane in figures 7-a,b (for a subsonic case with $U_\infty = 300$ m/s). Results given in figure 7-a correspond to an error calculated in the acoustic domain only, and can also illustrate the observed trends for a supersonic TBL which are not so different than those seen in the subsonic case (the inclusion of k_c in the acoustic domain make the calculation of $\epsilon^c_{\hat{p}\hat{p}}$ useless for a supersonic case). Beyond a value of $\Delta_x/\lambda_0 = 0.5$ and at a given planes separation (with the exception of values of spacing $h/\lambda_0 < 0.5$), the reproduction error monotonously increases.

For a spatial sampling below $\Delta_x/\lambda_0 = 0.5$ (i.e. at least 2 acoustic sources per acoustic wavelength) and a constant plane separation (say $h/\lambda_0 = 1$), small variations of the reproduction error are seen. If the spatial sampling is fixed (under the value of $\Delta_x/\lambda_0 = 0.5$, say 0.4), the reproduction error slightly increases with planes separation. Aucejo *et al* [5] also found that planes spacing has small effects on TBL reproduction with values between $\lambda_0/6$ and $2\lambda_0$, with poorest results for the higher spacing attributed to ill-conditioning of the problem. In the present work and as seen in figure 3-b in the DAF case, the fact that reproduction error increases with planes spacing is attributed to the narrowing of the reproduced wavenumber content.

Concerning subsonic TBL (low Mach number flows), many

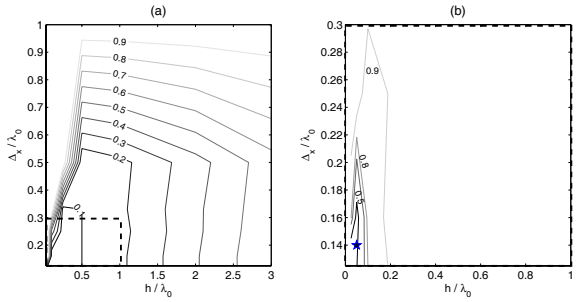

Figure 7: Reproduction error as a function of planes separation h and source separation Δ_x – (a) Error ϵ^0_{pp} calculated up to k_0 and (b) Error ϵ^c_{pp} calculated up to k_c.

works [1, 2] have shown that both convective and acoustic components contributions should be taken into account to study the vibroacoustic response of TBL-excited panels. This theoretically implies the reproduction of evanescent components (in contrast to propagating components in the acoustic domain) with small correlation scales, which physically requires nearfield sources and higher source densities than in the acoustic case [4, 5]. To extend the analysis to the specific reproduction of a subsonic TBL, a focus is made on a zone concerning only small plane spacings and high source densities (dashed box in figure 7-a). In figure 7-b, the calculated reproduction error $\epsilon^c_{\hat{p}\hat{p}}$ is always close to 1 (a 100 % error) except when $\Delta_x/\lambda_0 < 0.2$ and $h/\lambda_0 < 0.1$ (i.e. at least 5 monopoles per acoustic wavelength, with planes spaced by less than one tenth of an acoustic wavelength). This shows that the reproduction of a subsonic TBL up to the convective number with an acceptable reproduction error ($< 50\%$) seems feasible. Figures 8-a-d show the results obtained in terms of spatial CSD and CSD wavenumber spectrum, with parameters corresponding to the star plotted in figure 7-b ($\Delta_x/\lambda_0 \approx 0.14$ and $h/\lambda_0 = 0.05$). In figure 8-a,b (and compared to figure 5-a,b), correlation scales are now better reproduced in both streamwise and crosswise directions, even though reproduced amplitudes are nearly a quarter of the targeted amplitude. In the wavenumber domain (figure 8-c), a peak is reproduced for $k_x/k_0 \approx 1.6$, but with a lower magnitude than the targeted one. The level of the corresponding convective peak is nevertheless higher than the maximum of the reproduced acoustic part.

For the reproduction of subsonic TBL, Maury and Bravo [4] found that at least 3.7 monopoles per correlation length were needed, and Aucejo [5] obtained a value of at least 4 monopoles per smallest wavelength (even if they are not referred to the same quantity, their two results are quite equivalent as explained in [3]). In the presented results, the value of $\Delta_x/\lambda_0 \approx 0.14$ corresponds to 7 monopoles per acoustic wavelength. The corresponding number of acoustic sources per corresponding convective wavelength λ_c (i.e. to reproduce wavenumber up to k_c) can be obtained by simply multiplying this value by the ratio $k_0/k_c (= 0.6)$, which leads to a value of 4.3 monopoles per convective wavelength. This value is coherent with the results previously cited.

6 Towards a practical application

For the experimental testing of panels, reaching such a density of sources requires small sized transducers, with inherent limitations in low frequency and potentially in terms

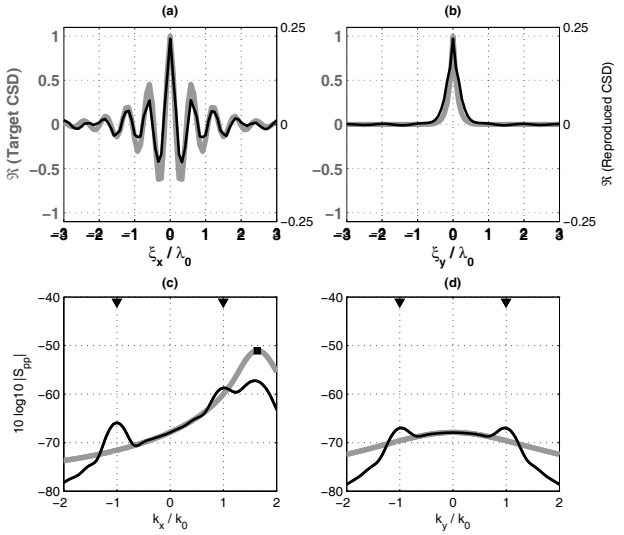

Figure 8: Subsonic TBL with $\Delta_x = 0.14\lambda_0$ and $h = \lambda_0/20$ – Target CSD and reproduced CSD in the $(\xi_x, 0)$ plane (a) and $(0, \xi_y)$ plane (b) – Target wavenumber-spectrum and reproduced wavenumber-frequency spectrum in the $(k_x, 0)$ plane (c) and $(0, k_y)$ plane (d).

of transducer sensitivity. Such limitations can be circumvented in different ways. Bravo and Maury [4] used the wavenumber filtering properties of the panel to be tested (reproducing panel vibration or sound pressure radiation instead of accurately reproducing the wall pressure fluctuations). This removes the technical constraint of a dense array, with an extended frequency range for the reproduction of TBL-induced vibration or noise. The *a priori* estimation of structural wavenumbers is nevertheless simple in the case of a uniform panel, but can be much complicated for panels with trims or stringers. The question of a dense source array can also be adressed using the concept of the synthetic antenna as suggested by Aucejo [5]. The synthetic antenna concept relies in the synthesis of a large and dense array, virtually constructed by moving a small antenna and using adapted signal processing (stationnarity hypothesis is clearly supposed in this approach, but so are the fields of interest). Moreover, the use of the synthetic antenna leads to better achieve an acoustically transparent source plane. This removes the potential problem of standing waves that is encountered with an array of baffled loudspeakers facing the panel to be tested. As Aucejo [5], we suggest for final laboratory applications to use a volume velocity source as a monopole source.

7 Conclusion

The presented simulation results show that sound field reproduction techniques for reproduction of spatially correlated sound fields seem promising. For both methods (WFS and P-NAH), the acoustic component of a DAF or a TBL can be reproduced with small errors, which leads to adequate reproduction of DAF and supersonic TBL. The present work leads to observations that are consistent with other studies [4, 5]. Whatever the random sound pressure field of interest might be, ensuring the reproduction of grazing plane waves implies that the size of the source plane should be at least equal to the reproduction plane (i.e. the size of a panel to be tested), and that source plane and reproduction plane should not be spaced by more than an acoustic wavelength (especially in the case of subsonic TBL to be able to include evanescent components). In the specific case of a subsonic TBL, the number of monopoles must also be refered to the smallest wavelength to be reproduced (i.e. at least the convective wavelength), with a value of 4.3 monopoles per convective wavelength here to obtain meaningful results.

One of the main advantages of the two presented frameworks is their open-loop schemes. If experimental conditions close to hemi-infinite space can be achieved (panel mounted in the rigid wall of a hemi-anechoic room), the complex amplitudes to be imposed to the reproduction sources can be easily determined *a priori*. Having defined the highest wavenumber to be reproduced (i.e. at least k_c and thus the convection speed U_c), this will define the number of monopoles to be used. The next step is to test both methods in a laboratory setup with a synthetic antenna approach.

Acknowledgments

This research has been supported by Bombardier Aerospace and the Natural Sciences and Engineering Research Council of Canada.

References

[1] B. Arguillat, D. Ricot, C. Bailly, G. Robert "Measured wavenumber : Frequency spectrum associated with acoustic and aerodynamic wall pressure fluctuations", *J. Acoust. Soc. Am.* **128** (4), 1647-1655 (2010).

[2] A. Borisyuk and V. Grinchenko, "Vibration and noise generation by elastic elements excited by turbulent flows", *J. Sound Vib.* **204**, 213-237 (1997).

[3] A. Berry, R. Dia, O. Robin, "A Wave Field Synthesis approach to reproduction of spatially-correlated sound fields", *J. Acoust. Soc. Am.* **131** (2), 1226-1239 (2012).

[4] T. Bravo, C. Maury, "A synthesis approach for reproducing the response of aircraft panels to a turbulent boundary layer excitation", *J. Acoust. Soc. Am.* **129** (1), 143-153 (2011).

[5] M. Aucejo, L. Maxit, J.-L. Guyader, "Utilisation d'une antenne synthétique pour simuler l'effet d'une couche limite turbulente", In Proc. of CFA 2010, Apr. 12-16 , Lyon, France (2010).

[6] G.M. Corcos, "The structure of the turbulent sound field on boundary-layer flows", *J. Fluid Mech.* **18**, 353-375 (1964).

[7] A. Berkhout, D. De Vries, P. Vogel, "Acoustic control by wave field synthesis", *J. Acoust. Soc. Am.* **36** (12), 2764-2778 (1993).

[8] E.G. Williams, *Fourier Acoustics : Sound radiation and nearfield acoustical holography*, Academic Press, San Diego (1999).